Wave-particle duality in tripartite systems

J. P. Marrou, C. Montenegro La Torre, M. Jara, and F. De Zela
Departamento de Ciencias, Sección Física
Pontificia Universidad Católica del Perú
Lima 15088, Peru

Quantum objects, sometimes called quantons, often display a characteristic feature that is referred to as wave-particle duality (WPD). Lately, this and other quantum traits have been submitted to intensive research, mainly motivated by the development of quantum information science. As a consequence, the scope of some concepts have been extended and it has been realized that they are not in the exclusive domain of quantum physics. This is particularly clear in optics, where qubits may show up as Jones vectors and WPD has its counterpart as wave-ray duality. WPD was originally addressed by focussing on a single qubit, which was afterwards supplemented with a second one playing the role of a path-marker in an interferometric setup. Fringe contrast, a sign of wave-like behavior, was proved to be diminished in connection with the effectiveness of the marker, the inducer of particle-like behavior. Going from bipartite to tripartite states is a natural and necessary step towards a better understanding of WPD. This step is what we have accomplished in this work. We report some constraints ruling WPD for tripartite systems, as well as their experimental display with single photons.

I. INTRODUCTION

As has been recently pointed out, "the quest for basic understanding is essential for further progress" in quantum information science [1]. Several questions concerning the foundations of quantum mechanics are being revisited and among these questions, those related to the essential meaning and scope of wave-particle duality (WPD) have motivated various studies, both theoretical and experimental ones. Many of the latter were designed to test quantifiers of WPD, such as visibility ($\mathcal{V}$) and distinguishability ($\mathcal{D}$). The scenario in which $\mathcal{V}$ and $\mathcal{D}$ are introduced is an interferometric setup, either identical or at least akin to the archetypical (optical) Young setup. Typically, one deals in these cases with three intensity measurements, I_a, I_b, I_c, when using classical light, or probability measurements when working with single photons. In either case, the mathematical description can be given in terms of a two-dimensional vector space with orthonormal basis $\{|\varphi_a\rangle, |\varphi_b\rangle\}$. We can thus write $|\varphi_c\rangle = c_a |\varphi_a\rangle + c_b |\varphi_b\rangle$ for a general vector, $c_{a,b}$ being complex coefficients. It should be stressed that usage of Dirac notation does not imply a quantum interpretation. In a two-arm interferometer, the coefficients $c_{a,b}$ carry information about the phases that are accumulated along each path and that can give rise to an interferogram, i.e., $c_i = d_i \exp(i\phi_i)$. Intensity or probability measurements can be given in terms of the c_i, as $I_i = \langle |c_i|^2 \rangle$. Angular brackets denote the corresponding, statistical or quantal, averaging procedure. Distinguishability and visibility are naturally defined as

$$\mathcal{D} := \frac{|I_a - I_b|}{I_a + I_b}, \qquad \mathcal{V} := \frac{I_c^{\max} - I_c^{\min}}{I_c^{\max} + I_c^{\min}}. \tag{1}$$

That is, $\mathcal{D}$ measures how distinguishable paths a and b are in terms of the corresponding intensities or probabilities that are associated to each of them. As for $\mathcal{V}$, it is defined in terms of $I_c = [I_a + I_b + 2|\langle c_a^* c_b \rangle| \cos(\arg\langle c_a^* c_b \rangle + \delta)]/2$, where δ is the relative phase-shift between $|\varphi_a\rangle$ and $|\varphi_b\rangle$. On varying δ, one obtains the maximal and minimal intensities that enter the definition of $\mathcal{V}$, which is thus a measure of fringe contrast.

The above quantifiers, $\mathcal{V}$ and $\mathcal{D}$, of WPD were shown [2–6] to be constrained by the inequality

$$\mathcal{D}^2 + \mathcal{V}^2 \leq 1. \tag{2}$$

Later on, this inequality was shown to follow from a tight constraint, which was established in the so-called polarization-coherence theorem (PCT) [7–10]:

$$\mathcal{D}^2 + \mathcal{V}^2 = \mathcal{P}^2, \tag{3}$$

where $\mathcal{P} \leq 1$ is the degree of polarization

$$\mathcal{P} := \frac{|\lambda_+ - \lambda_-|}{\lambda_+ + \lambda_-}. \tag{4}$$

Here, $\lambda_\pm$ are the eigenvalues of the 2×2 matrix, whose elements are $\langle c_i^* c_j \rangle$, with $i, j \in \{a, b\}$. The above definitions apply whenever we deal with two-state systems, or "qubits", which accumulate a relative phase. It is moreover assumed that we can measure, directly or indirectly, all the quantities that are defined in terms of vector amplitudes.

As inequality (2) shows, the more distinguishable the two paths are, the less visible is the interferogram. This complementarity between particle-like (or ray-like) features and wave-like features is at the core of WPD. The latter has been widely seen as a typical trait of quantum objects, or quantons. A way to acquire which-way information is to put a "marker" on one of the paths of the interferometer. To this end, one can use an additional degree of freedom (DOF) that the quanton might have besides its path DOF. By using an appropriate device on one path, one can vary the additional DOF, thereby putting a mark on the quanton. In the case of photons, the additional DOF can be polarization. Hence, one has a second qubit besides the qubit that is associated to the two-way alternative.

When dealing with two-qubit states, $|\Phi\rangle$, its constituents can be entangled. Entanglement is often quantified with concurrence, which is defined as $\mathcal{C}(\Phi) = |\langle\Phi|\widetilde{\Phi}\rangle|$ [11]. Here, $|\widetilde{\Phi}\rangle = (\sigma_2 \otimes \sigma_2)|\Phi^*\rangle$, with $|\Phi^*\rangle$ being the complex-conjugate of $|\Phi\rangle$ in the computational basis $\{|00\rangle, |01\rangle, |10\rangle, |11\rangle\}$, while σ_2 is the Pauli matrix having the eigenvectors $(|0\rangle \pm i\,|1\rangle)/\sqrt{2}$. The reduced, 2×2 density matrices, $\rho_1 = \mathrm{Tr}_2\,|\Phi\rangle\langle\Phi|$ and $\rho_2 = \mathrm{Tr}_1\,|\Phi\rangle\langle\Phi|$ have the same eigenvalues $\lambda_\pm$, and so also the same degree of polarization, given by Eq. (4), with $\lambda_+ + \lambda_- = 1$. One can readily find that $\mathcal{C}(\Phi) = 2\sqrt{\lambda_+\lambda_-}$. Thus, as a consequence of $\mathcal{P} = |\lambda_+ - \lambda_-|$ and $\lambda_+ + \lambda_- = 1$, we get $\mathcal{C}^2 + \mathcal{P}^2 = 1$. We can therefore write (3) in a form that holds for both ρ_1 and ρ_2, and which is known as the "triality relation" [12, 29]:

$$\mathcal{D}^2 + \mathcal{V}^2 + \mathcal{C}^2 = 1. \tag{5}$$

Both (3) and (5) have been submitted to experimental tests with all-optical setups [14, 15]. These tests, and the constraints they addressed, have extended the original, intuitive meaning of WPD. For instance, the qubit that was introduced to serve as a marker for the quanton, ended up being the qubit for which the constraint (2) was shown to hold true [5]. Later on, other constraints were derived, effectively involving two qubits [16, 17]. These constraints may be interpreted as disclosing the presence of hidden coherences that manifest themselves through their corresponding visibilities. It is then natural to ask what happens when one includes a third qubit. Tripartite states can have properties that differ from those of bipartite states, as for instance entanglement has shown. With this motivation, we have addressed tripartite states and derived some constraints that we have put to test in experiments with single photons. In what follows, we present said constraints and report the results of the corresponding, experimental tests.

II. THEORETICAL RESULTS

A. Constraints for concurrence and polarization with tripartite states

We will focus on pure, three-qubit states, given by

$$|\psi_{abc}\rangle = \sum_{i,k,m} d_{ikm}|a_i\rangle \otimes |b_k\rangle \otimes |c_m\rangle. \tag{6}$$

Let us first summarize some results that hold for such a general, tripartite state [18]. In terms of the density operator $\rho_{abc} = |\psi_{abc}\rangle\langle\psi_{abc}|$, we define the single-qubit subsystem $\rho_a = \mathrm{Tr}_{bc}(\rho_{abc})$, the two-party subsystem $\rho_{a(bc)} = \mathrm{Tr}_a(\rho_{abc})$, and similarly for the other cases. We further define the degree of polarization $\mathcal{P}_k = \sqrt{1 - 4\,\mathrm{Det}\rho_k}$ $(k = a, b, c)$. When dealing with two-party subsystems like $\rho_{a(bc)}$, it may occur that subsystem a gets entangled with subsystem bc, which is not a qubit. A measure for such an entanglement is given by the generalized concurrence ("I-concurrence") [19]

$$\mathcal{C}_{a(bc)} = \sqrt{2\left(1 - \mathrm{Tr}\,\rho^2_{a(bc)}\right)}. \tag{7}$$

Similar definitions apply to $\rho_{b(ac)}$ and $\rho_{c(ab)}$. One can readily show that $\mathrm{Tr}\,\rho^2_{a(bc)} = \mathrm{Tr}\,\rho^2_a$. It is then possible to reduce our case to the single-qubit case and make use of $\mathcal{P}^2_a = 1 - 4\,\mathrm{Det}\,\rho_a$, $\mathcal{C}^2_a = 2(1 - \mathrm{Tr}\,\rho^2_a)$ and $\mathrm{Tr}\,\rho_a = 1$, to obtain $\mathcal{C}^2_a + \mathcal{P}^2_a = 3 - 4\,\mathrm{Det}\,\rho_a - 2\,\mathrm{Tr}\,\rho^2_a = 3 - 2(\mathrm{Tr}\,\rho_a)^2 = 1$, and similar results for the other cases. Thus, we have the constraints

$$\mathcal{C}^2_{a(bc)} + \mathcal{P}^2_a = 1, \tag{8}$$

$$\mathcal{C}^2_{b(ac)} + \mathcal{P}^2_b = 1, \tag{9}$$

$$\mathcal{C}^2_{c(ab)} + \mathcal{P}^2_c = 1. \tag{10}$$

B. Wave-particle duality in tripartite states

In order to address WPD in the case of tripartite states, let us consider an initial state of the form

$$\rho_{abc}^{(i)} = |\psi_{ab}\rangle\langle\psi_{ab}| \otimes |0_c\rangle\langle 0_c|, \tag{11}$$

$$|\psi_{ab}\rangle = a_1 e^{i\phi_1}|0_a 0_b\rangle + a_2 e^{i\phi_2}|0_a 1_b\rangle + a_3 e^{i\phi_3}|1_a 0_b\rangle + a_4 e^{i\phi_4}|1_a 1_b\rangle. \tag{12}$$

The state $\rho_{abc}^{(i)}$ can be experimentally implemented by considering that a and b represent polarization DOFs, whereas c represents a path DOF. While a and b represent the same DOF, namely polarization, what distinguishes one from the other is that they belong to two different photons. Qubits b and c belong instead to one and the same photon. We further assume that we submit the bc-subsystem to a controlled-U transformation, given by

$$U_{bc} = [\sigma_0]_b \otimes |0_c\rangle\langle 0_c| + [U]_b \otimes |1_c\rangle\langle 1_c|, \tag{13}$$

where σ_0 stands for the 2×2 identity matrix, c is the control-qubit and b is the target-qubit. The a-qubit remains unchanged, so that the three-qubit transformation is $[\sigma_0]_a \otimes U_{bc}$. As a result, we obtain the tripartite, final state

$$\rho_{abc}^{(f)} = ([\sigma_0]_a \otimes U_{bc}) \left(\rho_{abc}^{(i)}\right) ([\sigma_0]_a \otimes U_{bc})^\dagger . \tag{14}$$

For each single-qubit state with density matrix ρ_k $(k = a, b, c)$, we define visibility and distinguishability as before. In terms of the matrix elements $\rho_{i,j}$, the corresponding definitions lead to the expressions [20]

$$\mathcal{V}(\rho) = \frac{2|\rho_{12}|}{\rho_{11} + \rho_{22}}, \qquad \mathcal{D}(\rho) = \frac{|\rho_{11} - \rho_{22}|}{\rho_{11} + \rho_{22}}. \tag{15}$$

On considering the degree of polarization $\mathcal{P} = \sqrt{1 - 4\mathrm{Det}\rho}$ in each case, as well as $\mathrm{Tr}\,\rho = 1$, one gets

$$4|\rho_{12}^{(a)}|^2 + \left(\rho_{11}^{(a)} - \rho_{22}^{(a)}\right)^2 = \mathcal{P}_a^2 = 2\ \mathrm{Tr}\,\rho_{a(bc)}^2 - 1, \tag{16}$$

$$4|\rho_{12}^{(b)}|^2 + \left(\rho_{11}^{(b)} - \rho_{22}^{(b)}\right)^2 = \mathcal{P}_b^2 = 2\ \mathrm{Tr}\,\rho_{b(ac)}^2 - 1, \tag{17}$$

$$4|\rho_{12}^{(c)}|^2 + \left(\rho_{11}^{(c)} - \rho_{22}^{(c)}\right)^2 = \mathcal{P}_c^2 = 2\ \mathrm{Tr}\,\rho_{c(ab)}^2 - 1. \tag{18}$$

Thus, in each case one recovers the equality $\mathcal{V}^2 + \mathcal{D}^2 = \mathcal{P}^2$, which can also be written in the form

$$\mathcal{V}^2(\rho_c) + \mathcal{D}^2(\rho_c) = 2\ \mathrm{Tr}\,\rho_{c(ab)}^2 - 1, \tag{19}$$

and similarly for the other cases.

C. Experimental display of wave-particle duality in tripartite states

Equation (19) corresponds to a case that is experimentally accessible with a Mach-Zehnder-type interferometer (MZI). A polarized photon that is submitted to this MZI carries both the polarization-qubit b and the path-qubit c. A second photon, which may serve to herald detections of the first one, carries polarization-qubit a. Qubits a and b may be entangled. Equation (19) shows that $\mathcal{V}(\rho_c)$ and $\mathcal{D}(\rho_c)$ are constrained by the purity of the state $\rho_{c(ab)}$, which is measured by $\mathrm{Tr}\,\rho_{c(ab)}^2$. Hence, this purity restricts the manifestation of WPD that we assign to the photon, whose quanton-qubit (the path-qubit) is represented by ρ_c. This is because the photon's polarization-qubit b may be seen as a path-marker, while the path-qubit c represents the quanton. The degree of polarization of qubit b depends, in turn, on how entangled this qubit is with qubit a. Complete polarization $(P = 1)$ cannot be achieved when a state is entangled with another one. The same holds for purity. As we will see below, the roles of marker and quanton can be interchanged. It is a matter of convention, which DOF is dubbed "marker" and which one is dubbed "quanton".

The MZI essentially consists on an input beam-splitter (BS), an output BS, and a phase-shifter between the two BSs. The unitary transformation that is performed by the BS on the path-qubit can be represented by $U_{\mathrm{BS}} = (\sigma_2 + \sigma_3)/\sqrt{2}$, where $\sigma_{k=2,3}$ stand for Pauli matrices. We can then set $U_{\mathrm{BS}}^{(bc)} = [\sigma_0]_b \otimes [U_{\mathrm{BS}}]_c$ for the BS action on the photon entering the MZI. A controlled-U transformation that is mounted on the MZI can then be specified by

$$U_{bc}(\theta) = e^{i\phi}[\sigma_0]_b \otimes |0_c\rangle\langle 0_c| + [\exp(i\theta\,\sigma_2)]_b \otimes |1_c\rangle\langle 1_c|, \tag{20}$$

where ϕ is the relative, adjustable phase of the unbalanced interferometer, and we have chosen $U_b(\theta) = \exp(i\,\theta\,\sigma_2)$ as the controlled U-transformation. For the unitary that acts on the tripartite state, we have then

$$U_T^{(abc)} = [\sigma_0]^{(a)} \otimes U_{MZ}^{(bc)}, \tag{21}$$

$$U_{MZ}^{(bc)} = U_{\rm BS}^{(bc)}\, U_{bc}(\theta)\, U_{\rm BS}^{(bc)}, \tag{22}$$

$$U_{\rm BS}^{(bc)} = [\sigma_0]_b \otimes [U_{\rm BS}]_c, \tag{23}$$

$$U_{\rm BS} = \frac{1}{\sqrt{2}}(\sigma_2 + \sigma_3). \tag{24}$$

Let us consider now the initial, two-qubit polarization state

$$|\psi_{ab}\rangle = \cos\alpha |H_a\rangle|H_b\rangle + \sin\alpha |V_a\rangle|V_b\rangle, \tag{25}$$

where $H(V)$ refers to horizontal (vertical) polarization. $|\psi_{ab}\rangle$ is thus a generally entangled, Bell-type state. Photon a is the heralding or idler photon. Its twin photon carries two qubits, the polarization-qubit b and the path-qubit c. This photon is submitted to the action of a MZI, which has two retardation plates mounted on one of its arms. The retardation plates are two half-wave plates (H), conveniently oriented so as to implement the unitary $U_b(\theta)$:

$$U_b(\theta) = \exp(i\,\theta\,\sigma_2) = H\left(\frac{\pi - \theta}{2}\right) H(0). \tag{26}$$

The initial polarization state of the signal photon is $\rho_b^{(i)} = {\rm Tr}_{ac}\, \rho_{abc}^{(i)}$, where $\rho_{abc}^{(i)}$ is given by (11), with the state $|\psi_{ab}\rangle$ chosen as above, see (25). We set $\rho_b^{(U)} = U_b(\theta)\rho_b^{(i)}U_b^\dagger(\theta)$. As has been shown when addressing the two-qubit extension of the polarization-coherence theorem [21], the distinguishability and visibility that belong to the b-qubit are given by

$$\mathcal{D}_b = \frac{1}{2}\left|\rho_b^{(U)} - \rho_b^{(i)}\right| = |\cos(2\alpha)||\sin\theta|, \tag{27}$$

$$\mathcal{V}_b = \left|{\rm Tr}\left(U(\theta)\rho_b^{(i)}\right)\right| = |\cos\theta|. \tag{28}$$

Moreover, we have that

$$\mathcal{P}_a = \sqrt{1 - 4\det\rho_a} = |\cos(2\alpha)|, \tag{29}$$

which, as already mentioned (see Eq. (8)), satisfies $\mathcal{C}_{a(bc)}^2 + \mathcal{P}_a^2 = 1$. Here, the generalized concurrence $\mathcal{C}_{a(bc)}$ is given by

$$\mathcal{C}_{a(bc)} = \sqrt{2\left(1 - {\rm Tr}\,\rho_{a(bc)}^2\right)} = \sqrt{2\,(1 - {\rm Tr}\,\rho_a^2)}. \tag{30}$$

On considering (27,28,29), we obtain the following constraints for visibility and distinguishability of the photon's b-qubit, the photon that is submitted to the MZI:

$$\mathcal{V}_b^2 + \mathcal{D}_b^2 = \mathcal{P}_a^2 \sin^2\theta + \cos^2\theta, \tag{31}$$

$$\mathcal{V}_b^2 + \mathcal{D}_b^2 + \mathcal{C}_{a(bc)}^2 \sin^2\theta = 1. \tag{32}$$

We notice that, in this case, it is the polarization b-qubit the one which plays the role of a quanton, i.e., the one displaying WPD. Qubits a and c do enter the above constraints, but they do not have clearly identifiable roles as markers. In principle, the roles of quanton and marker can be conventionally assigned to one or the other qubit. However, what matters is the constraint that $\mathcal{V}$ and $\mathcal{D}$ are submitted to, as a manifestation of WPD. Interchanging the roles of quanton and marker requires, of course, changing from one to other experimental setup. We show next how this can be accomplished.

III. DESIGN OF EXPERIMENTAL TESTS AND MEASUREMENT RESULTS

A. Polarization-qubit as a quanton

In the previous section, we addressed the case in which the polarization b-qubit is the one that plays the role of quanton. The corresponding MZI-type setup, which is the one we used in our experimental tests, is shown in Fig. (1).

Our goal was to test the constraint (32) in two cases. First, we took $\alpha = \pi/6$ and varied θ and, second, we fixed $\theta = 11\pi/36$ and varied α. The fixed values were chosen so as to have clearly distinguishable curves (see Fig. (3)).

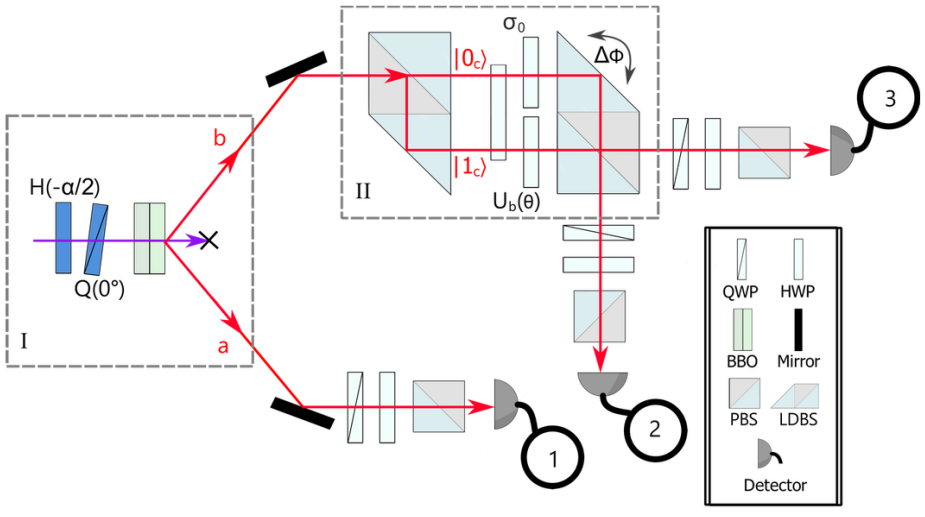

FIG. 1: Experimental setup for polarization-qubit as a quanton. Part I: generation of the polarization-entangled photons by spontaneous parametric down conversion. Part II: Mach-Zehnder type interferometer. Unboxed part: Measurement and detection devices. Coincidences are registered between any pair of the labeled detectors. HWP: half-wave plate. QWP: quarter-wave plate. BBO: paired beta-barium borate crystals. LDBS: lateral displacement 50-50 beam-splitter. PBS: polarizing beam-splitter. $\Delta\phi$ indicates the relative phase between both paths controlled by the tilt of the last LDBS.

In our setup, polarization-entangled photons of 800 nm wavelength were generated by spontaneous parametric down conversion (SPDC) in a pair of beta-barium borate (BBO) crystals, which were set face to face and having their optical axes oriented perpendicularly to one another. A cw-laser of 400 nm wavelength (0.7 nm linewidth, 37.5 mW) was used to pump the BBO crystals and so produce photon pairs in a type-I process, i.e., the two photons, a and b, had the same polarization, orthogonal to that of the pump field. Following the standard procedure to generate entangled photons [22], the pump polarization was adjusted with a half-wave plate (HWP) and with a tilted quarter-wave-plate (QWP), so as to produce, by SPDC, the desired, initial two-photon state (see Eq. (25)).

Next, photon b was submitted to the sequence of a LDBS, three HWPs and another LDBS, which together constitute the MZI that was referred to in the previous section. The unitary $U_b(\theta)$ was implemented with two HWPs in the configuration $H(0)H(\frac{\pi-\theta}{2})$ These HWPs were mounted on the displaced path of the first BS. The absorption effect of the HWPs was compensated with two HWPs set to zero on the transmitted path.

To measure $\mathcal{V}_b^2$, we removed the sequence Q-H-PBS before detectors 1 and 3 (see Fig. (1)). Then, we recorded a pair of maximum and minimum values of coincidence counts between both detectors. By tilting the last LDBS (see Fig 1), we varied the optical-path difference between the arms of the interferometer. To obtain $\mathcal{D}_b^2$, we removed the setup for polarization projection before detector 1 and measured the difference of the Stokes vectors associated to each arm of the interferometer. The vectors were determined by single-qubit polarization tomography, after blocking one of the outputs in the first LDBS. For this tomographic procedure, we measured the number of coincidences between detectors 1 and 3, after setting the angles of the Q-H-PBS device before detector 3 so as to project on the relevant polarization components. The Stokes vector of the displaced path was used to estimate the experimental value of $\sin\theta$. We obtained $\mathcal{C}_{a(bc)}^2$ from the experimental reconstruction of density matrix ρ_a. To measure the polarization state of photon a, we removed the Q-H-PBS gadgets before detectors 2 and 3, and performed the single-qubit polarization tomography, as in the case of $\mathcal{D}_b^2$, only that this time we obtained the relevant polarization projections with the setup before detector 1, and we measured the sum of coincidences on detectors 1-2 and 1-3. This amounts to incoherently superpose the two beams of the last LDBS in the MZI, to be jointly detected afterwards, so that any information about the path of photon b is erased. Idler and signal photons, a and b respectively, were detected with single-photon counting modules (SPCMs). The synchronized avalanche photodetectors registered coincidences within a time-window of 10.42 ns.

In order to diagnose the accuracy with which we produced the initial polarization-entangled states (see Eq. (25)), we performed quantum state tomography [23] and calculated the fidelity $\mathcal{F}(\rho_{ab}^{(i)}, \rho_{ab-\mathrm{exp}}^{(i)}) = \mathrm{Tr}\sqrt{(\rho_{ab}^{(i)})^{1/2}\rho_{ab-\mathrm{exp}}^{(i)}(\rho_{ab}^{(i)})^{1/2}}$

of the produced state $\rho^{(i)}_{ab-\mathrm{exp}}$ with respect to the target state $\rho^{(i)}_{ab}$. We also recorded $\mathrm{Tr}(\rho^{(i)}_{ab})^2$ as a measure of the state's purity. Typical values were, e.g., $\mathcal{F}(\rho^{(i)}_{ab}, \rho^{(i)}_{ab-\mathrm{exp}}) = 0.972$ and $\mathrm{Tr}(\rho^{(i)}_{ab})^2 = 0.902$, in the case of the state given by Eq. (25), with $\alpha = \pi/6$. In Fig. (2), we show a typical record of the density matrix $\rho^{(i)}_{ab-\mathrm{exp}}$.

Fig. (3) shows our results concerning Eq. (32) for fixed $\alpha = \pi/6$ and varying θ and for fixed $\theta = 11\pi/36$ and varying α. While in the two cases there is good agreement between theory and experiment, the second case shows a better agreement. This reflected the accuracy of the alignments and plate orientations that were involved in one and the other case.

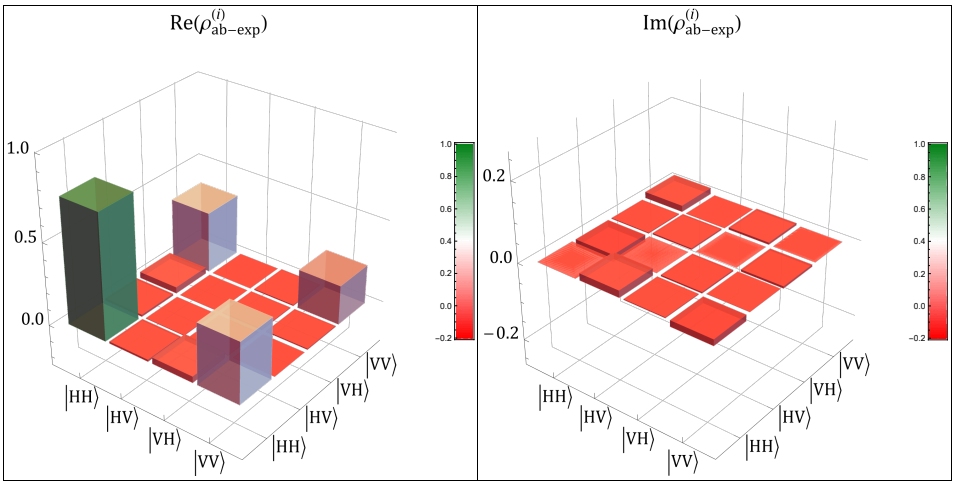

FIG. 2: Real and imaginary parts of the density matrix of a pure state $|\psi_{ab}\rangle$ with $\alpha = \pi/6$ (see Eq. (25)). The measured purity and fidelity were 0.902 and 0.972, respectively.

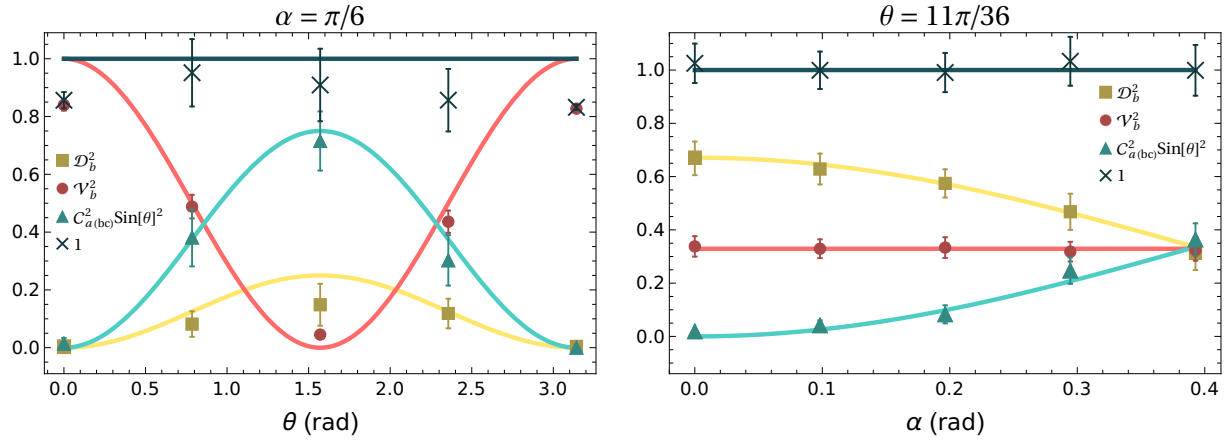

FIG. 3: Experimental test of the constraint given by Eq. (32) in the text. Left panel: The value of α remains fixed while θ varies as shown in the figure. Right panel: Parameter θ is held fixed, and α varies as shown in the figure.

B. Path-qubit as a quanton

As already said, the roles of quanton and marker are interchangeable. The original aim in [5] was to couple the quanton to another system that serves as a which-way marker (or "detector"). Polarization and spin are typical examples for such an additional DOF that the quanton may carry and be used as a marker. However, the constraint between $\mathcal{V}$ and $\mathcal{D}$ that was obtained in [5] referred to the marker, not to the quanton. This illustrates that WPD may manifest itself in different ways, and that its original meaning must be extended in many respects.

Here we show how the path DOF can retake its role as a quanton. To this end, our setup must be changed a little bit. Figure (4) shows how it looks. The input BS of the MZI-type setup has been replaced by a polarizing beam-splitter (PBS) and the two HWPs are now set on path $|0_c\rangle$, one before and the other after the PBS. Additionally, another HWP is set on path $|1_c\rangle$ to compensate the absorption effect. In what follows, we explain the theoretical description of the new setup.

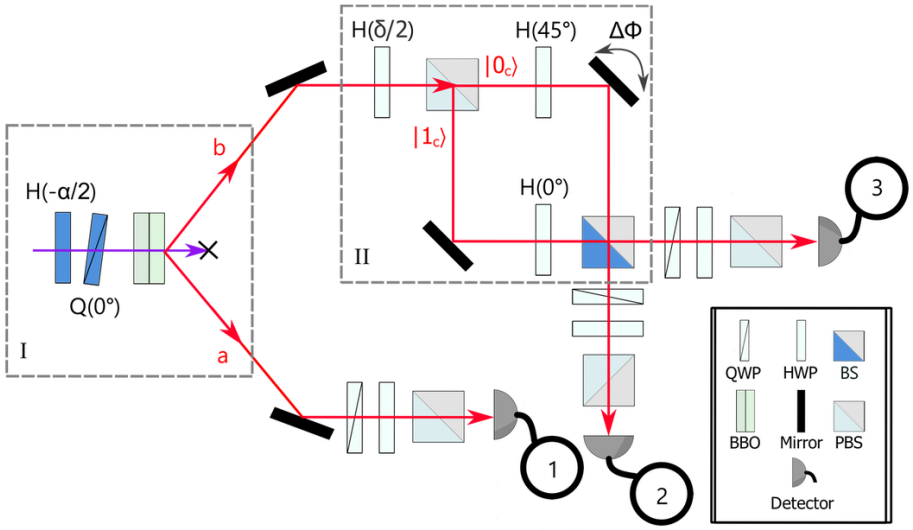

FIG. 4: Experimental setup for path-qubit as a quanton. Part I: generation of the polarization-entangled photons by spontaneous parametric down conversion. Part II: Mach-Zehnder type interferometer. Unboxed part: Measurement and detection devices. Coincidences are registered between any two detectors. HWP: half-wave plate. QWP: quarter-wave plate. BBO: paired beta-barium borate crystals. PBS: polarizing beam-splitter. BS: 50-50 beam-splitter. $\Delta\phi$: relative phase between paths, which is controlled by tilting the mirror.

The initial state is also in this case given by (11) and (25). That is,

$$\rho_{abc}^{(i)} = |\psi_{ab}\rangle\langle\psi_{ab}| \otimes |0_c\rangle\langle 0_c|, \tag{33}$$

$$|\psi_{ab}\rangle = \cos\alpha|H_a\rangle|H_b\rangle + \sin\alpha|V_a\rangle|V_b\rangle. \tag{34}$$

The MZI-type setup performs now the following unitary transformations.

$$U_T^{(abc)} = [\sigma_0]^{(a)} \otimes U_{MZ}^{(bc)}, \tag{35}$$

$$U_{MZ}^{(bc)} = U_{\rm BS}^{(bc)}\, U_{bc}(\delta), \tag{36}$$

$$U_{\rm BS}^{(bc)} = [\sigma_0]_b \otimes [U_{\rm BS}]_c, \tag{37}$$

$$U_{bc}(\delta) = \left[\, e^{i\phi} H_b(\pi/4) \otimes |0_c\rangle\langle 0_c| + H_b(0) \otimes |1_c\rangle\langle 1_c| \,\right] U_{\rm PBS}^{(bc)} \left[\, H_b(\delta/2) \otimes [\sigma_0]_c \,\right], \tag{38}$$

$$U_{\rm BS} = (\sigma_2 + \sigma_3)/\sqrt{2}, \tag{39}$$

$$U_{\rm PBS}^{(bc)} = |H_b\rangle\langle H_b| \otimes [\sigma_0]_c + |V_b\rangle\langle V_b| \otimes [\sigma_1]_c, \tag{40}$$

where ϕ represents again the relative phase between both paths. Before the output-BS in the MZI, the tripartite system is in the state

$$\rho_{abc}^{(\delta)} = U_\delta^{(abc)} \rho_{abc}^{(i)} \left(U_\delta^{(abc)}\right)^\dagger, \tag{41}$$

where $U_\delta^{(abc)} = [\sigma_0]_a \otimes U_{bc}(\delta)$. After the BS, the tripartite system is in the state

$$\rho_{abc}^{(f)} = U_T^{(abc)} \rho_{abc}^{(i)} \left(U_T^{(abc)}\right)^\dagger. \tag{42}$$

On considering the path-state $\rho_c^{(\delta)} = \mathrm{Tr}\,\rho_{abc}^{(\delta)}$, its visibility and distinguishability can be calculated using Eqs. (15) with $\mathrm{Tr}\,\rho = 1$, i.e., $\mathcal{V} = 2|\rho_{12}|$ and $\mathcal{D} = |\rho_{11} - \rho_{22}|$. As for the degree of polarization, it is given by

$$\mathcal{P}_c^2 = 2\,\mathrm{Tr}\left(\rho_{c(ab)}^{(f)}\right)^2 - 1, \tag{43}$$

where $\rho_{c(ab)}^{(f)} = \mathrm{Tr}_c\,\rho_{abc}^{(f)}$. One readily gets

$$\mathcal{V}_c^2 = \cos^2(2\alpha)\sin^2(2\delta), \tag{44}$$
$$\mathcal{D}_c^2 = \cos^2(2\alpha)\cos^2(2\delta), \tag{45}$$
$$\mathcal{P}_c^2 = \cos^2(2\alpha). \tag{46}$$

We have therefore,

$$\mathcal{V}_c^2 + \mathcal{D}_c^2 = \mathcal{P}_c^2 = 2\,\mathrm{Tr}\left(\rho_{c(ab)}^{(f)}\right)^2 - 1. \tag{47}$$

To test the above constraint, we set $\delta = \pi/10$ and varied α. We obtained the quantities entering the constraint as follows. $\mathcal{V}_c^2$ was obtained with the same procedure that was used for getting $\mathcal{V}_b^2$. As for $\mathcal{D}_c^2$, it was obtained by measuring the normalized difference between coincidence counts of detectors 1-2 (for transmitted path) and detectors 1-3 (for displaced path). To obtain $\rho_{c(ab)}$, which fixes the right-hand side of (47), we performed a coincidence measurement which is similar to the one explained in relation to $\mathcal{C}_{a(bc)}^2$, only that this time we needed the information about the polarization of photons a and b. Hence, sequences Q-H-PBS were held in place before detectors 2-3 and we performed two-qubit polarization tomography [23].

Our test of constraint (47) shows good agreement between theory and experiment, as can be seen in Fig. (5) and in Table (I). Differences between theory and experiment are attributable to inaccuracies in the alignment of optical elements and in the plates' orientation. Constraint (47) refers to the path DOF that has been traditionally considered when referring to WPD. The photon's polarization is an additional DOF, which does not show up explicitly in (47), but indirectly contributes to its establishment. It is worth stressing that such an indirect contribution does not promote the polarization DOF to be a which-way marker. It is however possible to retrieve which-way information from the polarization DOF, as recently shown [24], though the tested constraints are then simpler than the ones we have addressed here.

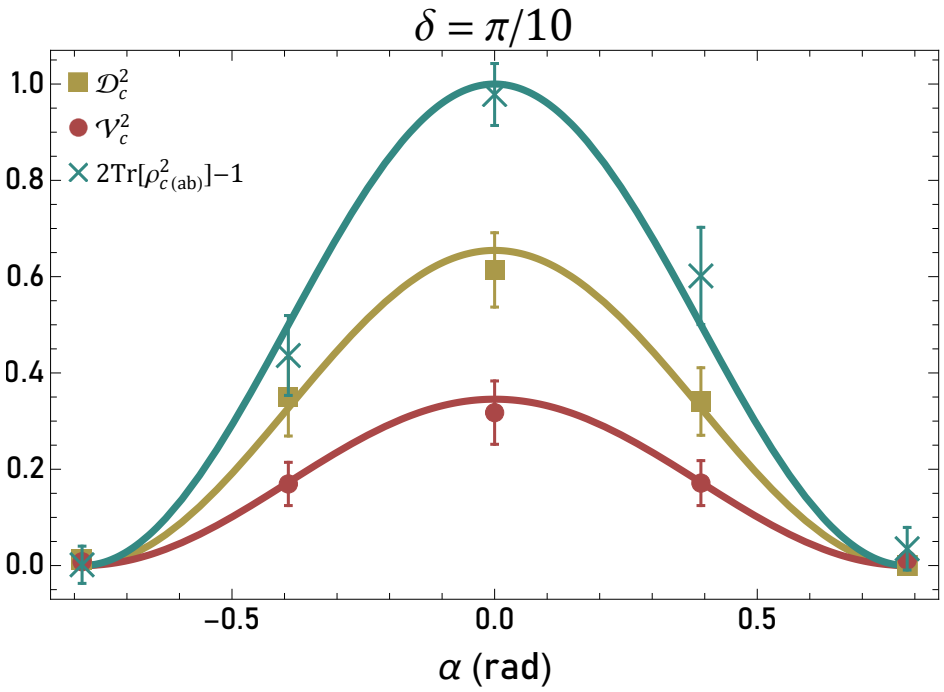

FIG. 5: Experimental test of the constraint given by Eq. (47). Parameter δ is held fixed, and α varies as shown in the figure.

$\alpha\,(^\circ)$	$\mathcal{V}_c^2+\mathcal{D}_c^2$	$2\,\mathrm{Tr}\left(\rho_{c(ab)}^{(f)}\right)^2-1$
-45	0.02 ± 0.01	0.00 ± 0.04
-22.5	0.52 ± 0.09	0.44 ± 0.08
0	0.93 ± 0.10	0.98 ± 0.06
22.5	0.51 ± 0.08	0.60 ± 0.10
45	0.01 ± 0.01	0.04 ± 0.04

TABLE I: Experimental test of the constraint given by Eq. (47). We compare the experimental values of the two sides of the equation, for different values of α (see Eqs. (44), (45), (46)).

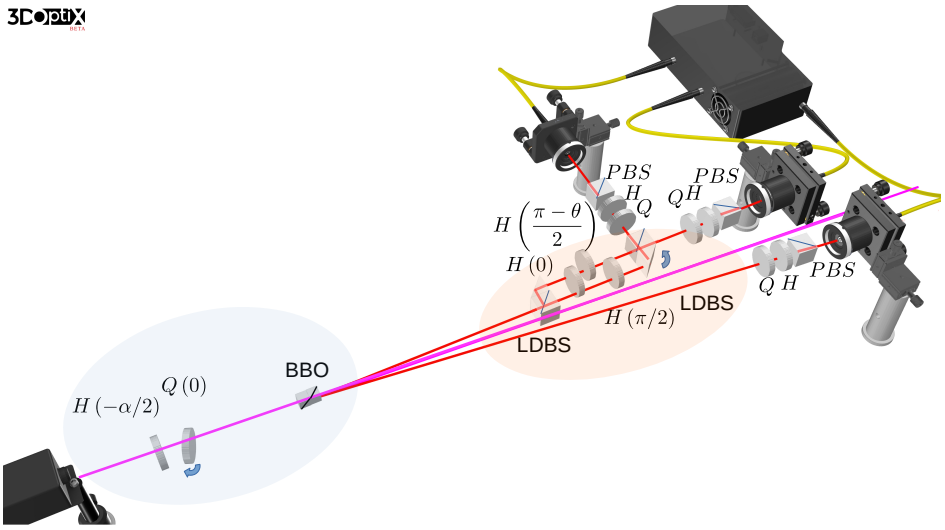

FIG. 6: Realistic representation of our experimental setup for the case in which the polarization-qubit is the quanton. The light blue and light orange regions correspond, respectively, to Part I and part II in Fig. (1).

IV. SUMMARY AND CONCLUSIONS

We report various constraints that rule wave-particle duality (WPD). These constraints were derived by addressing tripartite states of three qubits. Two of these qubits correspond to the polarization degree of freedom of two entangled photons and the third one corresponds to the path degree of freedom of one of the photons. By considering various subsystems of one and two qubits, it is possible to derive constraints for visibility and distinguishability, features commonly used to quantify wave-like and particle-like behavior, respectively, of the physical object that is supposed to exhibit WPD, the so-called quanton. The idea of using one DOF as a which-way marker has led in the past to the establishment of some constraints. We have derived new ones and submitted them to experimental tests. Our approach shows that the roles of quanton and marker are interchangeable, meaning that a given qubit can play any of these roles, depending on the experimental context. We believe that our results contribute to gain additional insight into the meaning of WPD. This meaning, as illustrated by recent studies [25–29], should be extracted from both the actual mathematical definitions of the quantifiers of WPD and the operational definition of the observables being measured in the corresponding, experimental tests.

Funding. We acknowledge financial support from the European Commission, Grant Number H2020-MSCA-RISE-2019-872049; FONDECYT, Grant Number 236-2015 and DFI-PUCP, Grant Number PI0882.

Disclosures. The authors declare no conflicts of interest.

Data availability. Data underlying the results presented in this paper are not publicly available at this time but may be obtained from the authors upon reasonable request.

[1] I. H. Deutsch, "Harnessing the power of the second quantum revolution", Phys. Rev. X Quantum **1**, 020101 (2020).
[2] W. K. Wootters and W. H. Zurek, "Complementarity in the double-slit experiment: Quantum nonseparability and a quantitative statement of Bohr's principle," Phys. Rev. D **19**, 473 (1979).
[3] D. M. Greenberger and A. Yasin, "Simultaneous wave and particle knowledge in a neutron interferometer," Phys. Lett. A **128**, 391 (1988).
[4] G. Jaeger, A. Shimony, and L. Vaidman, "Two interferometric complementarities," Phys. Rev. A **51**, 54 (1995).
[5] B.-G. Englert, "Fringe visibility and which-way information: An inequality," Phys. Rev. Lett. **77**, 2154 (1996).
[6] M. Jakob and J. A, Bergou, "Complementarity and entanglement in bipartite qudit systems," Phys. Rev. A **76**, 052107 (2007).
[7] M. Jakob and J. A, Bergou, "Quantitative complementarity relations in bipartite systems: Entanglement as a physical reality," Opt. Commun. **283**, 827 (2010).
[8] J. H. Eberly, X.-F. Qian, and A. N. Vamivakas, "Polarization coherence theorem," Optica **4**, 1113 (2017).
[9] A. F. Abouraddy, A. Dogariu, B. E. A. Saleh, "Polarization coherence theorem: comment," Optica, **6**, 829 (2019).
[10] J. H. Eberly, X.-F. Qian, and A. N. Vamivakas, "Polarization coherence theorem: reply," Optica, **6**, 831 (2019).
[11] W. K. Wootters, "Entanglement of Formation of an Arbitrary State of Two Qubits," Phys. Rev. Lett. **80**, 2245 (1998).
[12] X.-F. Qian, A. N. Vamivakas, J. H. Eberly, "Entanglement limits duality and vice versa," Optica **5**, 942 (2018).
[13] T. Qureshi, "Predictability, distinguishability, and entanglement," Opt. Lett. **46**, 492 (2021).
[14] X.-F. Qian, T. Malhotra, A. N. Vamivakas, and J. H. Eberly, "Coherence constraints and the last hidden optical coherence," Phys. Rev. Lett. **117**, 153901 (2016).
[15] X.-F. Qian, K. Konthasinghe, S. K. Manikandan, D. Spiecker, A. N. Vamivakas, and J. H. Eberly, "Turning off quantum duality," Phys. Rev. Res. **2**, R012016 (2020).
[16] F. De Zela, "Hidden coherences and two-state systems," Optica **5**, 243 (2018)
[17] F. De Zela, "Generalizing Wave-Particle Duality: Two-Qubit Extension of the Polarization Coherence Theorem," Quantum Reports **2**, 501 (2020).
[18] C. R. M. Montenegro La Torre, Y. Yugra, and F. De Zela, "Relationship between entanglement and polarization in tripartite states", J. Opt. **24**, 105202 (2022).
[19] P. Rungta, V. Buzek, C. M. Caves, M. Hillery, and G. J. Milburn, "Universal state inversion and concurrence in arbitrary dimensions", Phys. Rev. A **64**, 042315 (2001).
[20] M. Jara, J. P. Marrou, M. Uria, C. Montenegro La Torre, and F. De Zela, "Experimental display of generalized wave-particle duality", Opt. Expr. **30**, 34740 (2022).
[21] P. Sánchez, J. Gonzales, V. Avalos, F. Auccapuclla, E. Suarez, and F. De Zela, "Experimental display of the extended polarization-coherence theorem", Opt. Lett. **44**, 1052 (2019).
[22] P. G. Kwiat, E. Waks, A. G. White, I. Appelbaum, and P. H. Eberhard, "Ultrabright source of polarization-entangled photons", Phys. Rev. A **60**, R773 (1999).
[23] D. F. V. James, P. G. Kwiat, W. J.Munro, and A. G. White, "Measurement of qubits", Phys. Rev. A **64**, 052312 (2001).
[24] D-X. Chen, Y. Zhang, J-L. Zhao, Q-C. Wu, Y-L. Fang, C-P. Yang, and F. Nori, "Experimental investigation of wave-particle duality relations in asymmetric beam interference". npj Quantum Information, **8**, 1 (2022).
[25] A. Norrman, K. Blomstedt, T. Setälä, A. T. Friberg, "Complementarity and Polarization Modulation in Photon Interference," Phys. Rev. Lett. **119**, 040401 (2017).
[26] A. Norrman, A. T. Friberg, and G. Leuchs, "Vector-light quantum complementarity and the degree of polarization," Optica, **7**, 93 (2020).
[27] X.-F. Qian and G. S. Agarwal, "Quantum duality: A source point of view," Phys. Rev. Research **2**, 012031(R) (2020).
[28] T. H. Yoon and M. Cho, "Quantitative complementarity of wave-particle duality," Sci. Adv. **7**, eabi9268 (2021).
[29] T. Qureshi, "The delayed-choice quantum eraser leaves no choice," Int. J. Theor. Phys. **60**, 3076 (2021).